Urban Ecosystems (2026) 29:73
https://doi.org/10.1007/s11252-026-01935-3

RESEARCH

# Selenium bioaccumulation in industrialized urban forests: case study of five tree species used for phytoremediation

İsmail Koç[1] · Hakan Sevik[2] · Constantin Nechita[3] · Ugur Canturk[4] · Andreea Maria Iordache[5] · J. Julio Camarero[6]

Received: 1 September 2025 / Accepted: 15 February 2026 / Published online: 26 February 2026


**Abstract**

Heavy metal pollution poses significant risks to ecosystems and human health, necessitating effective monitoring and mitigation strategies. This study focused on the priority pollutant selenium (Se) content, evaluating five tree species (*Tilia tomentosa*, *Robinia pseudoacacia*, *Cedrus atlantica*, *Pseudotsuga menziesii*, and *Fraxinus excelsior*) to assess their capacity to biomonitor and mitigate Se in urban parks of Düzce (Türkiye). We quantified Se accumulation in the outer bark, inner bark, and wood across the four cardinal directions of the stem. Results showed striking inter-species variation: *R. pseudoacacia* and *C. atlantica* woods accumulated exceptionally high Se concentrations (91.9 and 77.4 mg·kg$^{-1}$, respectively), while *P. menziesii* and *F. excelsior* showed non-detectable levels. Strong directional effects were pronounced, e.g., with the north aspect in *C. atlantica* accumulating 2.7× higher Se than the east aspect (77.40 vs. 28.09 mg·kg$^{-1}$). Se was generally higher in bark than wood. *C. atlantica* is recommended for phytoremediation due to constrained inter-tissue translocation (e.g., north-south differential: 45.39 vs. 36.10 mg·kg$^{-1}$). In comparison, *R. pseudoacacia* showed high bioavailability but high variability by cardinal direction (66.40–91.92 mg·kg$^{-1}$). These findings reveal species-specific Se accumulation patterns influenced by microenvironmental factors, emphasizing the targeted use of *R. pseudoacacia* and *C. atlantica* for pollution monitoring and Se mitigation in urban areas.

**Keywords** Heavy metal · Selenium · Biomonitoring · Phytoremediation · Radial content

## Introduction

Atmospheric pollution under actual climate change is a major global issue, especially in industrialized and urban areas, affecting human and ecosystem health (Nechita et al. 2021; Guney et al. 2023; Koç et al. 2025a). The UN Environment Programme (UNEP) states that unhealthy environments result in around 12.6 million deaths annually. Over 66% of them are caused by fine particulate matter charged with organic and inorganic pollution (Carvalho 2021; Sevik et al. 2024). These facts underscore the urgent need for effective mitigation strategies to safeguard public

✉ İsmail Koç
ismailkoc@duzce.edu.tr

Hakan Sevik
hsevik@kastamonu.edu.tr

Constantin Nechita
constantin.nechita@icas.ro

Ugur Canturk
ugurcanturk55@gmail.com

Andreea Maria Iordache
andreea.iordache@icsi.ro

J. Julio Camarero
jjcamarero@ipe.csic.es

1 Department of Forest Engineering, Düzce University, 81620 Düzce, Türkiye

2 Department of Environmental Engineering, Kastamonu University, 37150 Kastamonu, Türkiye

3 Department of Biometry, National Institute for Research and Development in Forestry “Marin Drăcea”, Calea Bucovinei, 73 bis, Câmpulung Moldovenesc 725100, Romania

4 Institute of Science, Düzce University, Düzce 81620, Türkiye

5 National Research and Development Institute for Cryogenics and Isotopic, Technologies—ICSI Rm. Valcea, 4 Uzinei Street, Valcea 240050, Romania

6 Instituto Pirenaico de Ecología (IPE-CSIC), Avda. Montañana 1005, Zaragoza 50080, Spain

health and environmental sustainability (Yang et al. 2022; Beloconi and Vounatsou 2023). Highly industrialized countries with advanced technology can find solutions to reduce environmental pollution and recycle potentially toxic materials released into the environment (Jain 2024). In contrast, underdeveloped and developing nations struggle to prioritize and adequately tackle this critical issue (Uncumusaoğlu and Mutlu 2021; Isinkaralar et al. 2025a, b). However, studies worldwide indicate that the levels of heavy metals—considered the most hazardous pollutants for the environment and human health—continue to rise in soil, water, and air (Şimşek and Mutlu 2023; Swain 2024; Ayteğin and Özcan 2026) and have reached dangerous levels in many urban zones (Mutlu et al. 2024; Şevik et al. 2024). Metropolitan areas encounter elevated contamination levels from toxic chemical elements due to increased waste generation (Ziaeemehr et al. 2023). This contamination can be substantially influenced by atmospheric urban heating, which alters the behavior of chemicals under temperature variations (Irfeey et al. 2023; Nechita et al. 2025a, b). These combined effects lead to water and heat stress and various health issues (Ali et al. 2019; Iordache et al. 2022; Saxena 2025). The United States Environmental Protection Agency (U.S. EPA) has established health guidelines for selenium (Se) concentration in air at 0.02 mg/m$^3$. Elevated selenium (Se) concentrations in humans may lead to symptoms such as fever and nausea, as well as adverse effects on the liver, kidneys, and heart. In severe cases of toxicity, cardiac and pulmonary symptoms can occur and can lead to death (Hadrup and Ravn-Haren 2020).

In soil, Se concentrations range from 0.01 to 2.00 mg·kg$^{-1}$, with a global average of 0.40 mg·kg$^{-1}$. Soils with Se concentrations between 1 and 5000 mg·kg$^{-1}$ are considered seleniferous. Soil concentrations are highly variable and depend on site-specific characteristics, and their transfer to plants, animals, and humans depends on bioavailability characteristics for each plant species and individual (Liu et al. 2021). This is because heavy metals are uptake in plants directly through the air via leaves via stomata, from the soil through roots, or from stem sections (Cobanoglu et al. 2023). Heavy metals enter living organisms primarily via inhalation or the food chain (Gogoi et al. 2024).

Plant-based biomonitoring offers a low-cost, practical alternative to expensive, error-prone instruments or methods for long-term monitoring of environmental pollution. Annual tree rings are recognized as biomonitors since they provide retrospective data regarding changes in heavy metal concentrations over time (Nechita et al. 2025a; Pulatoglu et al. 2025; Vasconcellos et al. 2025). However, each tree has a different capacity to accumulate heavy metals in its radial and axial profile. Therefore, suitable biomonitor species for each heavy metal should be determined separately (Koc et al. 2024). Although numerous studies have been conducted on tracking heavy metal pollution, more focus has been on the more common elements such as Pb, Ni, Cr, Mn, and Cu (Isinkaralar et al. 2024; Balraju et al. 2025). Thus, various studies evaluated heavy metal content in various tree species, organs, and organelles, showing significant differences in assimilation (Aricak et al. 2019; Sevik et al. 2019a, b; Cesur et al. 2021; Erdem et al. 2023; Zeren Çetin 2024; Koç 2025). Health agencies, including the Agency for Toxic Substances and Disease Registry (ATSDR) and U.S. EPA, underscore research on high-risk elements due to their public and environmental risks, as is the case with Se (Sevik et al. 2024). Se plays vital physiological roles in organisms, and exhibits a dual behavior, ranging from beneficial to toxic (Huang et al. 2019; Ullah et al. 2023). The Earth's crust releases Se naturally through weathering processes, but human activities—particularly fossil fuel combustion, metallurgical operations, and intensive agriculture—have significantly amplified its environmental dispersion (Gan et al. 2021; Zou and Mauter 2021). This balance between nutritional needs and pollutant risks exists across ecosystems, as increasing Se levels in air, soil, and water pose new challenges for environmental and public health management (He et al. 2018; Ullah et al. 2023).

Despite its recognized toxicity, Se remains less studied than other heavy metals, underscoring the urgent need for research on monitoring and reducing urban Se contamination. This study addresses this gap by examining tree species' ability to accumulate airborne Se in Düzce Province, Türkiye, and by providing a nature-based method for environmental assessment and remediation. Thus, the aim is to (1) assess heavy metal assimilation pattern in radial transect and under four cardinal directions in outer bark, inner bark, and wood, (2) document temporal changes in metal content along tree rings, (3) identify the tree species with best performance for monitoring and mitigating Se under urban and environmental contamination. The current research investigates variations in Se accumulation among tree species under comparable soil and atmospheric conditions. The study aims to fill a gap in understanding Se absorption in tree tissues and will contribute novel knowledge to biomonitoring and phytoremediation in urban and industrial environments.

## Materials and methods

### Study site

Düzce province, situated in a low-lying basin (40°.90′ N, 31°.315′ E, 140 m a.s.l.) within Türkiye Western Black Sea region, experiences significant air quality challenges due to its unique geographical and meteorological conditions (Koç 2021; Çevre, Şehircilik ve İklim Değişikliği Bakanlığı 2023). The area's bowl-shaped topography, surrounded by mountain ranges, restricts pollutant dispersion. This effect is amplified by the local climate, which features mild winters (average 12.5 °C), hot summers (maximum 30 °C in August), and a mean annual precipitation of 540 mm since 1950 (Fig. 1). The climate extracted from the E-OBS v31.0e climatic grid (Haylock et al. 2008) indicates that both temperature and precipitation increased after 1985 in the region, and the climatic diagram shows a typical Mediterranean climate with winter rains. Since 1992, the mean temperature has risen from 12 to 14.7 °C. The precipitation pattern shows a relatively flat trend from 1990 to 2010, with an average of 576 mm/year, followed by a sudden increase to 694 mm/year.

Heavy metals in the air bind to particulate matter, thereby serving as a sink for these pollutants. Therefore, as particulate matter levels rise in polluted areas, air concentrations of heavy metals also increase (Liu et al. 2025; Matei et al. 2025). This contamination with heavy metals becomes most severe in late autumn and winter, with PM2.5 concentrations peaking at 47.7 µg/m³ (November) and 49.9 µg/m³ (December) (IQAir 2024). During these months, coal combustion increases, and frequent temperature inversions occur, both of which intensify pollution by disrupting the mixing and dispersion of pollutants in the atmosphere. Autumn-winter precipitation increases atmospheric deposition to soil and vegetation, increasing the amounts while also enhancing dilution and absorption. Combining these human-made and natural factors creates an ongoing air quality issue that needs targeted mitigation strategies focused on emission sources and the area's specific weather vulnerabilities. The study location, topographical features, and sample map location are illustrated in Fig. 2.

## Sample preparation and element analysis

### Sample collection

The tree stem slice samples were collected from five species, including *Robinia pseudoacacia* L., *Tilia tomentosa* Moench, *Cedrus atlantica* (Endl.) Manetti ex Carrière, *Fraxinus excelsior* L. and *Pseudotsuga menziesii* (Mirb.) Franco. All the tree species mentioned are commonly used in urban and natural landscaping in the Düzce region, where they occur naturally and through human planting. Three trees (and thus three stem discs) were sampled per species. The sample size, although limited by the availability of appropriate mature samples within the urban park environment, is justified for several reasons. The primary objective of this study was to identify significant, species-specific differences in selenium accumulation potential under consistent pollution exposure. The chosen trees were the only individuals that met the strict criteria of similar age, health, and size within the study site. They were growing in a homogeneous stand with nearly identical soil characteristics, slope, and aspect. This environmental consistency reduces variability within species, making it easier to identify clear comparative trends. Additionally, the comprehensive sampling approach offers significant intra-tree replication: from each of the three trees, samples were collected from four cardinal

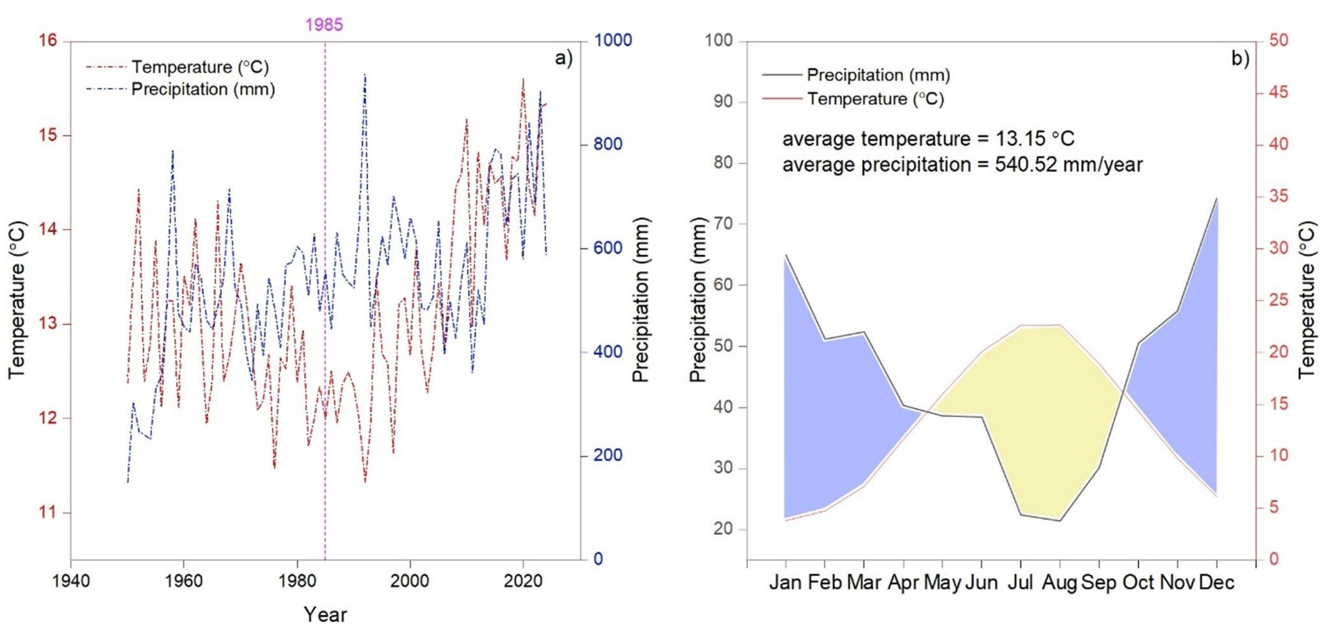


**Fig. 1** Climatic data (mean monthly temperature and mean monthly precipitation) in the Düzce province since 1950 to the present (**a**) and climatic diagram (**b**)

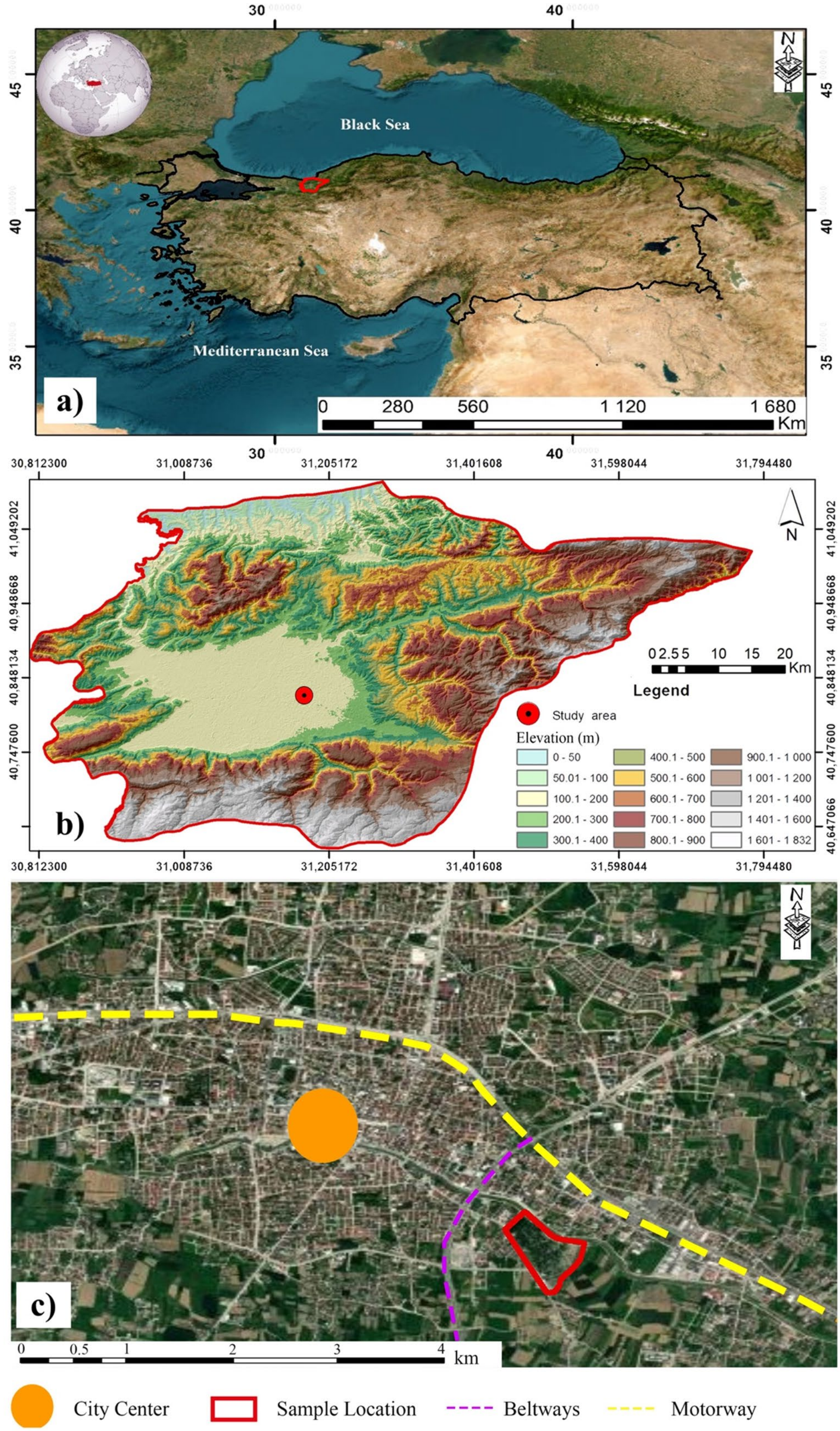


**Fig. 2** The study location (**a**) is situated in the southeastern part of Europe near the Black Sea, (**b**) the topographical features, and (**c**) the sample map location in Düzce, Türkiye

directions and three tissue types, with wood further divided into twelve age groups of five years each. The adopted methodology was used to obtain a high-resolution dataset comprising 2520 observational data points for robust statistical evaluation of patterns. This approach, which uses a smaller number of intensively sampled individuals to assess comparative accumulation, aligns with some dendrochemical studies (e.g., Cobanoglu et al. 2023; Sevik et al. 2024).

Selected trees were mature, healthy, spaced 5–10 m apart within rows, and of similar age, height, and diameter to ensure they were exposed to comparable levels of pollution. The age, diameter, and height range values of the trees included in the study are given in Table 1. Log samples were obtained from the stem at approximately 50±10 cm above ground level after the vegetation season ended in 2022, with a thickness of 10±5 cm. The entire cross-sectional discs were then used to measure along four compass directions (East, South, West, and North). The trees were 20–25 m tall, had a diameter of 40–55 cm, and were 60 years old. The randomly selected trees were planted in rows approximately 20 m apart. This way, the trees' branches and roots would not interfere with one another or impede airflow between them.

## Sample preparation and conducting Se analyses

To prepare the wood samples for analysis, cross-sectional discs were sanded to enhance the visibility of annual growth rings. The sanding process was conducted in a dedicated clean area on a disposable plastic sheet to prevent contamination from underlying surfaces. Residual dust generated during sanding was removed using clean, compressed air and soft, non-abrasive brushes, working systematically from the bark toward the pith to avoid redistributing surface contaminants into the interior wood zones targeted for sampling. The entire cross-sectional discs were subsequently used to measure along four compass directions: East, South, West, and North. Comparable studies have categorized tree rings into age groups of 3, 5, and 10 years based on factors such as tree age and ring width. In our case, this classification was suitable for the 5-ring group, providing content that supported the initiation of chemical analysis (Key et al. 2023; Sevik et al. 2024; Isinkaralar et al. 2024). A steel drill was used to extract specimens from the wood (WD), inner bark (IB), and outer bark (OB) of all age clusters. Thus, we sampled five tree species, four directions, three stem slices (from different trees), 14 categories (12 age groups WD + 1 IB + 1 OB), and three replicates. Three replicates were obtained for each annual ring width, which were divided into 5-year groups (a total of 12 age groups). Between each sampling point (cardinal direction and tissue type), the drill bit was meticulously cleaned with ethanol and dried to prevent cross-contamination, and the disc surface was wiped with a clean, lint-free cloth to remove any residual dust. The complete sample collection dataset contains 2520 observations in triplicate and underwent a thorough diagnostic evaluation (Fig. 3). This method has been used in previous studies in this field (Erdem et al. 2024; Koç et al. 2025a; Kulac et al. 2025; Sevik et al. 2025). The collected material was ground into sawdust, stored in open glass containers, air-dried for 15 days, and then oven-dried at 45 °C for an additional week.

**Table 1** Age, diameter, and height range values of the trees included in the study

| Species | Age | Height (m) | Diameter ($d_{1.30}$) (cm) |
|---|---|---|---|
| *R. pseudoacacia* | 60 | 20–21 | 40–42 |
| *T. tomentosa* | 60 | 20–22 | 39–42 |
| *C. atlantica* | 60 | 20–21 | 50–52 |
| *F. excelsior* | 60 | 22–24 | 50–54 |
| *P. menziesii* | 60 | 24–25 | 53–55 |

For elemental analysis, 0.5 g of dried sample was digested with 6 mL of 65% $HNO_3$ and 2 mL of 30% $H_2O_2$ using microwave-assisted acid digestion (200 °C for 15 min ramp and 15 min hold). The digested solutions were brought to 50 mL with ultrapure water and analyzed by ICP-OES (GBC Scientific Equipment Pty Ltd., Melbourne, Australia) to quantify Se concentrations, adjusted for dilution factors.

## Statistical analysis

The normality was tested using the Kolmogorov-Smirnov test and one-way ANOVA with Levene's test to confirm variance homogeneity and differences between variances. Following these validation steps, we conducted post hoc Duncan tests to compare multiple means after the ANOVA indicated a significant difference ($p < 0.05$) between four compass directions. The fitting model with ANOVA statistics involves splitting total data variability (total sum of squares, SST) into explained variance (model sum of squares, SSM) and unexplained variance (error sum of squares, SSE) to assess if predictors affect the response, using an *F*-test and p-value, to investigate if the model fits better than a simple mean. We also used trend analysis and analysis of variance to assess whether the means of the four compass-direction groups (patterns across ordered levels of concentration and time) differed. This process involves rejecting the null hypothesis if $p < 0.05$ and conducting a polynomial contrast to decompose the significant variance in trend components. Notably, *F. excelsior* and *P. menziesii* samples showed Se concentrations below the detection limit in their annual rings (dry weight [d.w.] basis) and were therefore excluded from the final statistical analysis. The statistical analysis was performed using SPSS 22.0 environment. The ANOVA

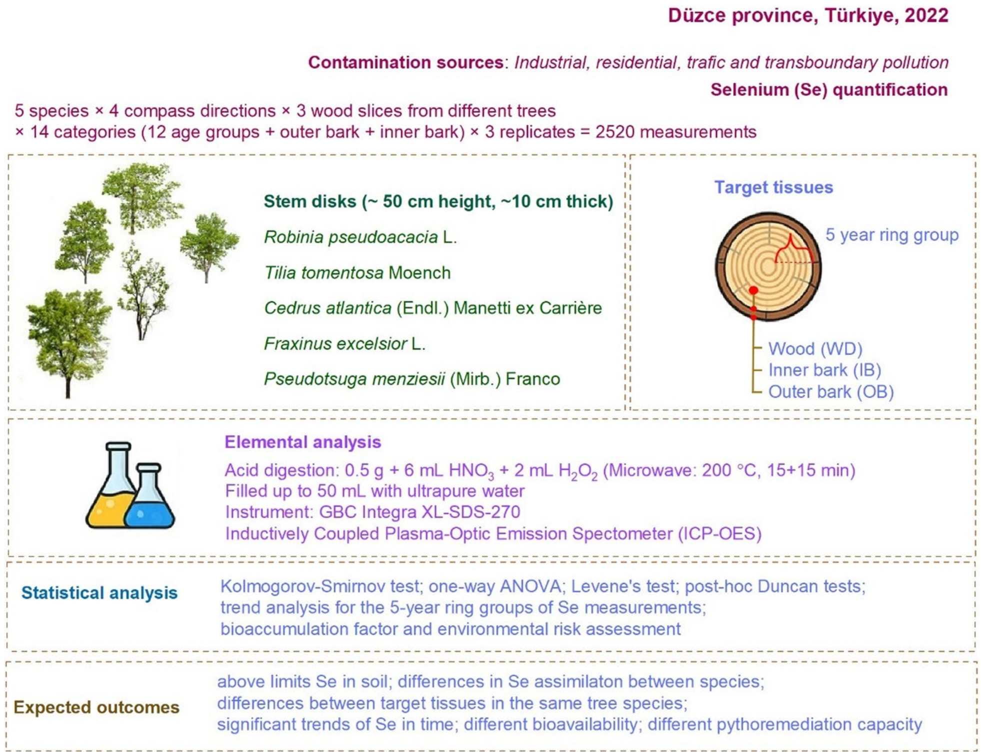


**Fig. 3** Methodological flowchart for the study, including samples used, target tissues, elemental analysis, statistical analysis, and expected outcomes

model partitions into distinct, independent polynomial trends, as summarized in Eq. 1.

$$Y_{ij} = \mu + \alpha_i + \epsilon_{ij} \quad (1)$$

were, $Y_{ij}$ are observed values modelled as the sum of the overall mean ( $\mu$ ) the effect of a specific group ( $\alpha_i$) and random error ( $\epsilon_{ij}$). The trend analysis with ANOVA involves the model sum of squares ($SS_{Model}$) decomposition into orthogonal trend components. F-trend represents the mean square for the trend divided by the error mean square (MSE) to test significance.

## Results

### Selenium content in tree organs and across cardinal directions

Non-detectable Se levels in both IB and WD tissues were documented in eastern-facing *T. tomentosa* samples (Table 2). The mean Se content across all tissues and directions was extremely low (0.87 mg·kg$^{-1}$), and in the eastern direction in IB and WD, it was below the detection limit. The OB exhibited directional variability, with peak concentrations in the north, followed by the south, and minimal accumulation in the western side of the trunk. When evaluating mean content values, a significant gradient emerged across tissues, with the lowest values in WD and progressively higher values in IB and OB (Fig. 4).

Content levels, which varied significantly when assessing cardinal directions and across all plant tissues ($p<0.05$), were observed in *R. pseudoacacia* (Table 2). This species had the highest Se content among the species, with a mean value of 77.04 mg·kg$^{-1}$ (across organs and directions) (Fig. 4). The highest Se concentrations consistently occurred in northern exposures, decreasing in the following order: north>south>east>west. Se content across tree organs shows distinct patterns of assimilation: OB>IB>WD (north), IB>OB>WD (east), OB>WD>IB (south), and IB>OB=WD (west). Only the eastward direction showed distinct organ-specific accumulation patterns; the other directions showed no statistically significant differences among tissues. Based on the mean Se concentration, there was no statistically significant variation among tissues ($p>0.05$).

*C. atlantica* Se content demonstrates significant variation across all tissues and within the order of assimilation (38.84 mg·kg$^{-1}$), which is nearly half the amount observed in *R. pseudoacacia* (Table 2). The mean Se content was comparable across the east, west, and south directions, whereas the north direction had a higher mean. Worth mentioning that in the north direction, the IB contained a value comparable to *R. pseudoacacia* (78.61 mg·kg$^{-1}$), indicating a high potential of Se assimilation for this species. IB exhibited the highest content compared to the WD and OB (Fig. 4). While organ-specific differences were generally not statistically significant between the east and west directions, differences were observed ($p>0.05$).

**Table 2** Mean (±standard deviation) and maximum selenium content (mg·kg$^{-1}$ d.w.) in different organs of the five species across cardinal directions

| Species | Tissue | North | | East | | South | | West | | F-value | Mean |
|---|---|---|---|---|---|---|---|---|---|---|---|
| | | Mean | Max | Mean | Max | Mean | Max | Mean | Max | | |
| *T. tomentosa* | OB | 1.96±0.11 cD | 2.07 | 0.99±0.03 B | 1.02 | 1.23±0.08 cC | 1.29 | 0.58±0.06 bA | 0.63 | 179.5*** | 1.19±0.53 c |
| | IB | 0.96±0.10 bB | 1.05 | < B.D.L. | - | 1.09±0.05 bC | - | 0.86±0.07cA | 0.93 | 6.7* | 0.97±0.12 b |
| | WD | 0.38±0.10 a | 0.58 | < B.D.L. | - | 0.38±0.09 a | 0.65 | 0.35±0.08 a | 0.54 | 0.5 ns | 0.37±0.09 a |
| | F-value | 393.8*** | | – | | 200.7*** | | 200.7*** | | – | 134.4*** |
| | Mean | 0.53±0.44 A | | 0.99±0.03 B | | 0.51±0.31 A | | 0.42±0.16 A | | 3.1* | – |
| *R. pseudoacacia* | OB | 88.02±0.55 C | 88.34 | 74.04±2.21 aB | 76.44 | 76.48±2.70 B | 79 | 69.85±0.27 A | 70.1 | 57.8*** | 77.10±7.20 |
| | IB | 87.77±0.01 C | 87.77 | 77.85±0.54 bB | 78.47 | 74.52±2.89 AB | 77.3 | 71.41±1.46 A | 72.7 | 8.6* | 77.89±6.56 |
| | WD | 86.17±8.62 D | 94.15 | 72.86±2.17 aB | 76.37 | 75.62±2.33 C | 79.4 | 69.99±2.92 A | 76.5 | 74.6*** | 75.49±7.23 |
| | F-value | 0.1 ns | | 7.8** | | 0.5 ns | | 0.3 ns | | – | 0.3 ns |
| | Mean | 87.32±7.80 D | | 73.30±2.45 B | | 75.60±2.35 C | | 70.08±2.75 A | | 92.5*** | – |
| *C. atlantica* | OB | 35.19±1.05 aB | 35.91 | 34.45±0.51 B | 34.84 | 36.86±0.22 bC | 37.1 | 32.96±0.65 A | 33.7 | 17.2** | 34.87±1.58 a |
| | IB | 78.61±0.49 bC | 79.08 | 32.75±0.69 A | 33.19 | 34.63±0.39 aB | 34.9 | 34.56±1.18 B | 35.5 | 2638.7*** | 45.14±20.21 b |
| | WD | 43.48±15.43 aB | 78.83 | 32.67±1.64 A | 34.46 | 36.16±1.16 bA | 37.6 | 33.77±3.08 A | 36.3 | 13.0*** | 36.60±8.99 a |
| | F-value | 8.7** | | 1.7 ns | | 3.4* | | 0.2 ns | | – | 4.4* |
| | Mean | 45.39±17.17 B | | 32.52±1.59 A | | 36.10±1.17 A | | 33.77±2.88 A | | 17.5*** | – |
| *P. menziesii* | OB | 0.52±0.10 A | 0.52 | 1.04±0.15 bB | 1.20 | 0.62±0.09 A | 0.71 | 0.70±0.07 bA | 0.77 | 14.2** | 0.72±0.22 b |
| | IB | < B.D.L. | - | 0.47±0.06a | 0.52 | < B.D.L. | - | 0.48±0.08 a | 0.56 | 0.0 ns | 0.47±0.06 a |
| | WD | < B.D.L. | - | < B.D.L. | - | < B.D.L. | - | < B.D.L. | - | – | < B.D.L. |
| | F-value | – | | 25.3*** | | – | | 13.3* | | – | 6.9* |
| | Mean | 0.52±0.10 | | 0.75±0.33 | | 0.62±0.09 | | 0.59±0.14 | | 0.9 ns | – |
| *F. excelsior* | OB | 2.20±0.04 C | 2.24 | 1.76±0.02 bB | 1.77 | 1.58±0.17 B | 176 | 0.43±0.11 A | 0.56 | 163.5*** | 1.49±0.69 |
| | IB | < B.D.L. | - | 1.02±0.05 a | 1.06 | < B.D.L. | - | < B.D.L. | - | – | 1.02±0.05 |
| | WD | < B.D.L. | - | < B.D.L. | - | < B.D.L. | - | < B.D.L. | - | – | < B.D.L. |
| | F-value | – | | 11.4*** | | – | | – | | – | 0.4 ns |
| | Mean | 2.20±0.04 B | | 1.40±0.41 A | | 1.58±0.17 A | | 0.43±0.11 A | | 3.9* | – |

OB: Outer bark; IB: Inner bark; WD: Wood. B.D.L: Below detection limit. Statistical significance between mean values is highlighted by different letters. Lowercase letters (a, b, c, …) indicate significant differences between tissues, while uppercase letters (A, B, C, …) indicate significant differences between cardinal directions. The three levels of significance were presented as $p \leq 0.001$ (***), $p \leq 0.01$ (**), $p \leq 0.05$ (*), and not significant ($p > 0.05$ (ns).

A low Se content was assimilated by *P. menziesii* regardless of organs and cardinal directions (0.63 mg·kg$^{-1}$), noting that the content in WD tissues and IB samples from northern and southern directions had values below detection limits (Table 2). OB accumulation was substantially lower than in other species (Fig. 4), with maximum concentrations observed in eastern exposures. Duncan's grouping analysis ($\alpha = 0.05$) classified the remaining directional exposures (north, south, west) into a single homogeneous subset, indicating no statistically significant difference in Se concentrations across these directions.

A reduced Se accumulation capacity (1.39 mg·kg$^{-1}$) and a higher proportion of values below the detection limit across all species were also observed in *F. excelsior* (Table 2). The northern direction showed an accumulation peak of 2.20 ± 0.04 mg·kg$^{-1}$. Se content in all WD tissues and non-eastern IB samples remained below detection limits. OB tissues showed values above the detection limit (Fig. 4), whereas WD showed values below the detection limit, with distinct western exposures exhibiting the lowest concentrations.

## Selenium variability in time in wood and across cardinal directions

Analysis of *T. tomentosa* WD revealed that Se content from IB to pith in the east direction differs significantly from the other three cardinal directions (Fig. 5). The proportion of variance explained by the ANOVA model is high

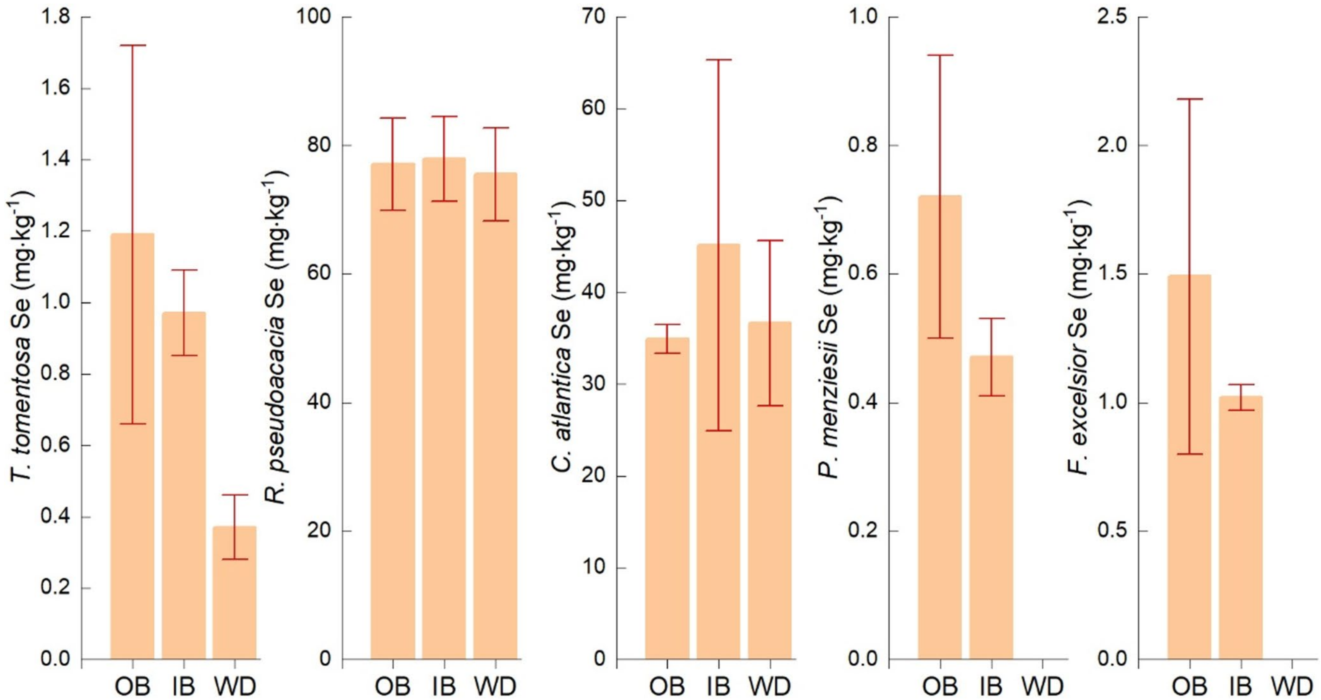


**Fig. 4** Mean species selenium content in wood (WD), inner bark (IB), and outer bark (OB), and standard deviation, for the five species investigated

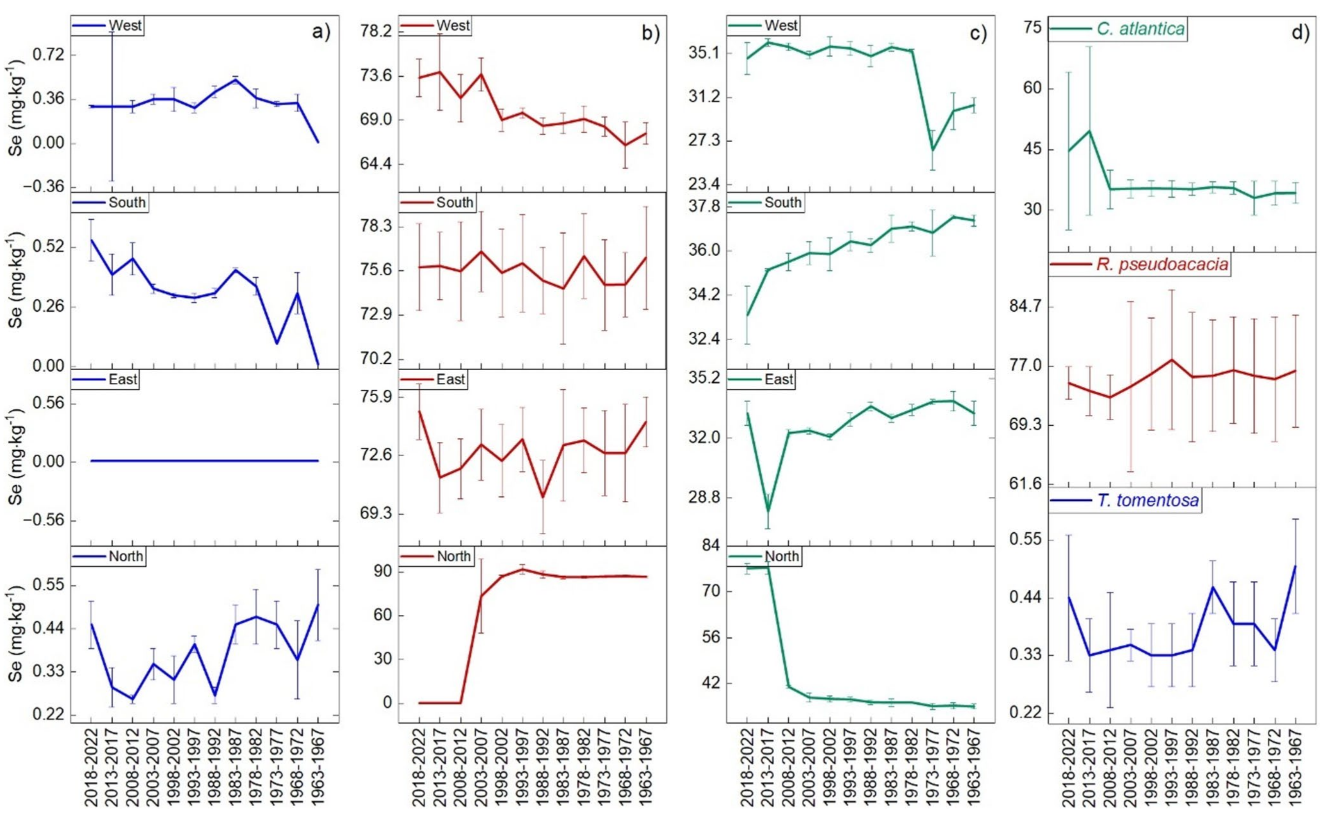


**Fig. 5** Temporal distribution of selenium content (mean ± standard deviation) for 5-year groups in (**a**) *T. tomentosa*, (**b**) *R. pseudoacacia*, (**c**) *C. atlantica* wood, and (**d**) average value for each species

($R$-squared = 0.73), indicating that the cardinal directions significantly account for the variation in Se content. The content in the radial profile of the stem, measured from the eastern side toward the pith, was below the detection limit. Trend analysis reveals a significant downward trend from the IB to the pith, specifically in the south direction ($p < 0.05$). In the north direction, the mean value for all decades (0.33 ± 0.09 mg·kg$^{-1}$) was comparable with the south (0.33 ± 0.13 mg·kg$^{-1}$), but the pattern of assimilation varied since 1992, when it increased in the north and decreased in the south. While directional variations were statistically insignificant ($p > 0.05$) in most sampling periods, significant differences ($p < 0.01$) did emerge during certain intervals, particularly between northern and southern exposures (Table 3). The overall stability of Se concentrations throughout the six-decade study suggests either limited atmospheric deposition or effective physiological regulation of Se uptake in woody tissues.

*R. pseudoacacia* showed no significant difference in mean Se content across various cardinal directions ($F$-value = 0.68, prob > $F$ = 0.56). However, the pattern of assimilation differs significantly, explaining the significant difference between cardinal directions variances ($F$-value = 29.00, prob > $F$ < 0.0001) (Fig. 5). In this case, the model fits the data poorly ($R$-squared = 0.04), indicating that the cardinal directions do not account for significant variability in Se content. The trend analysis revealed a significant upward trend from the IB to the pith and a downward trend to the west. The Se content in the west and south directions had no significant trends. Even so, measurements remained below detection limits in all north-direction samples from 2008 to 2022, whereas the highest value among all directions was observed between 2008 and 1973 (Table 4). Despite a general decreasing trend from West (69.99 mg·kg$^{-1}$) < East (72.86 mg·kg$^{-1}$) < South (75.62 mg·kg$^{-1}$) < North (86.17 mg·kg$^{-1}$) in mean values, a wide range was noted between extreme concentrations (max = 91.92 mg·kg$^{-1}$ vs. min = 66.40 mg·kg$^{-1}$).

The Se content in *C. atlantica* WD samples, when evaluated under cardinal directions, was found to vary significantly for both means west vs. north and east vs. north ($F$-value = 4.25, prob > $F$ < 0.01) and variance

**Table 3** Temporal and directional variations in selenium concentrations (mg·kg$^{-1}$ d.w) in *Tilia tomentosa* wood tissues

| Age cluster | North | East | South | West | F-value | Mean |
|---|---|---|---|---|---|---|
| 2018–2022 | 0.45±0.06 cdAB | < B.D.L. | 0.55±0.09 eB | 0.30±0.01 aA | 12.7** | 0.44±0.12 bcd |
| 2013–2017 | 0.29±0.05 a | < B.D.L. | 0.4±0.09 bcd | 0.30±0.61 aA | 4.1 ns | 0.33±0.07 ab |
| 2008–2012 | 0.26±0.01 aA | < B.D.L. | 0.47±0.07 deB | 0.30±0.05 aA | 16.4** | 0.34±0.11 a |
| 2003–2007 | 0.35±0.04 abc | < B.D.L. | 0.34±0.02 abc | 0.36±0.04 ab | 0.2 ns | 0.35±0.03 ab |
| 1998–2002 | 0.31±0.06 ab | < B.D.L. | 0.31±0.01 a | 0.36±0.10 ab | 0.7 ns | 0.33±0.06 a |
| 1993–1997 | 0.40±0.02 bcdB | < B.D.L. | 0.30±0.02 aA | 0.29±0.04 aA | 15.6** | 0.33±0.06 a |
| 1988–1992 | 0.27±0.02 aA | < B.D.L. | 0.32±0.02 abAB | 0.42±0.05 bcB | 14.6** | 0.34±0.07 a |
| 1983–1987 | 0.45±0.05 cd | < B.D.L. | 0.42±0.01 cd | 0.52±0.03 c | 6.7* | 0.46±0.05 cd |
| 1978–1982 | 0.47±0.07 d | < B.D.L. | 0.35±0.04 abc | 0.37±0.08 ab | 3.4 ns | 0.39±0.08 abc |
| 1973–1977 | 0.45±0.06 cdB | < B.D.L. | < B.D.L. | 0.32±0.02 abA | 12.6* | 0.39±0.08 abc |
| 1968–1972 | 0.36±0.10 abc | < B.D.L. | 0.32±0.09 ab | 0.33±0.07 ab | 0.2 ns | 0.34±0.06 a |
| 1963–1967 | 0.50±0.09 d | < B.D.L. | < B.D.L. | < B.D.L. | - | 0.50±0.09 d |
| F-value | 6.3*** | - | 9.1*** | 4.8** | | 3.4** |

**Table 4** Temporal and directional variations in selenium concentrations (mg·kg$^{-1}$ d.w) in *Robinia pseudoacacia* wood tissues

| Age cluster | North | East | South | West | F-value | Mean |
|---|---|---|---|---|---|---|
| 2018–2022 | < B.D.L. | 75.09±1.58 | 75.81±2.65 | 73.43±1.97 c | 1.0 ns | 74.78±2.11 |
| 2013–2017 | < B.D.L. | 71.36±1.98 | 75.89±2.06 | 74.01±3.98 c | 1.9 ns | 73.75±3.14 |
| 2008–2012 | < B.D.L. | 71.87±1.70 | 75.56±3.01 | 71.3±2.48 bc | 2.6 ns | 72.91±2.92 |
| 2003–2007 | 73.59±25.38 | 73.23±2.00 | 76.77±2.45 | 73.78±1.75 c | 0.0 ns | 74.34±11.03 |
| 1998–2002 | 87.06±0.94 C | 72.31±2.04 AB | 75.47±2.67 B | 69.01±1.16 abA | 54.9*** | 75.96±7.27 |
| 1993–1997 | 91.92±3.23 C | 73.53±1.81 AB | 76.06±2.97 B | 69.75±0.54 abA | 50.0*** | 77.81±9.06 |
| 1988–1992 | 88.53±2.51 C | 70.25±2.07 A | 75.00±2.03 B | 68.40±0.87 abA | 64.0*** | 75.54±8.40 |
| 1983–1987 | 86.57±0.94 C | 73.2±3.15 AB | 74.51±3.38 B | 68.68±1.06 abA | 30.0*** | 75.74±7.21 |
| 1978–1982 | 86.70±1.01 C | 73.46±1.82 B | 76.48±2.58 B | 69.12±1.39 abA | 51.8*** | 76.44±6.93 |
| 1973–1977 | 87.08±0.65 C | 72.75±2.40 B | 74.73±2.75 B | 68.33±1.01 abA | 52.3*** | 75.72±7.44 |
| 1968–1972 | 87.20±0.65 C | 72.75±2.76 B | 74.75±1.95 B | 66.40±2.42 aA | 51.0*** | 75.27±8.08 |
| 1963–1967 | 86.91±0.64 C | 74.51±1.41 B | 76.39±3.15 B | 67.62±1.11 aA | 56.5*** | 76.36±7.30 |
| F-value | 1.0 ns | 1.1 ns | 0.2 ns | 5.4*** | | 0.3 ns |

($F$-value = 10, prob > $F$ < 0.0001) (Fig. 5). The ANOVA fit model indicates low variability in metal content, with the cardinal directions accounting for 22% of the variance ($R$-squared = 0.22). The content from the IB to the pith exhibited an upward trend in the south and east directions, a downward trend in the north, and no significant trend in the west ($p < 0.05$). Temporal trends were segregated into two distinct groups using Duncan's test: pre-2012 and post-2013 periods, indicating a notable increase in Se accumulation in recent years (Table 5). Directional data were similarly clustered into two groups, with northern exposures forming a separate, higher-accumulation group (43.48 mg·kg$^{-1}$) distinct from other orientations (32.67–36.16 mg·kg$^{-1}$). The range between extreme concentrations was highest among all analyzed species (max = 77.40 mg·kg$^{-1}$; min = 26.47 mg·kg$^{-1}$). Particularly striking was the 2.7-fold disparity between adjacent north (77.40 mg·kg$^{-1}$) and east (28.09 mg·kg$^{-1}$) exposures during 2013–2017, demonstrating pronounced microenvironmental sensitivity and high potential to assimilate Se metallic content.

It is observed that some species undergo sudden fluctuations at different times (Fig. 5). For example, in *C. atlantica*, the Se concentration in the westward direction increased with age, with values during periods 1973–1977 > 1978–1982 > 2008–2012 > 2013–2017 (26.47 < 35.27 ~ 35.09 < 49.57 mg·kg$^{-1}$, respectively). The Se content on the eastern side ranged from 32 to 33 mg·kg$^{-1}$, indicating a decline during 2013–2017 (28.09 mg·kg$^{-1}$). In comparison, in the north, it increased from 41.03 mg·kg$^{-1}$ (2008–2012) to 77.40 mg·kg$^{-1}$ (2013–2017). The *R. pseudoacacia* ring groups had a Se concentration of 73.59 mg·kg$^{-1}$ during the 2003–2007 period, but remained below the detection limit in subsequent periods.

## Discussion

The study aimed to evaluate the capacity of five tree species to monitor and comprehend their ability to assimilate selenium (Se) in their organs from four cardinal directions. Statistical analysis revealed substantial differences in Se content between woody and bark tissues, underscoring their distinct sequestration capacities. It was demonstrated that the OB, IB, and WD of *T. tomentosa*, *P. menziesii*, and *F. excelsior* do not accumulate higher Se levels; furthermore, measurements were below the detection limit in some cases. The results suggest reduced atmospheric Se uptake or enhanced exclusion mechanisms in all three species (Liu et al. 2007; Winkel et al. 2015; Yuan et al. 2024). Particularly for *P. menziesii*, the highest Se accumulation of 1.04 mg·kg$^{-1}$ was observed in OB tissues oriented eastward, indicating limited uptake capacity and reduced atmospheric deposition retention compared to other species. Furthermore, the Se content of *T. tomentosa* was below detectable levels in the eastern direction. In contrast, *R. pseudoacacia* and *C. atlantica* showed high potential for Se absorption and assimilation.

The wood Se concentrations (max and min) measured in *R. pseudoacacia* and *C. atlantica* (66.40–91.92 mg·kg$^{-1}$ and 26.47–77.40 mg·kg$^{-1}$, respectively) provide critical context for local pollution levels. These concentrations far exceed the specific threshold values (generally < 1–2 mg·kg$^{-1}$) in plant tissues and are consistent with the ranges reported for vegetation in Se-rich or industrially affected areas (Winkel et al. 2015; Gan et al. 2021). The U.S. EPA health guideline for Se threshold in the air is 0.02 mg/m$^3$, underscoring its potency as a hazardous airborne pollutant. The high concentrations bioaccumulated in tree tissues suggest that historical atmospheric deposition in the area has been substantial. Therefore, the high bioaccumulation factors observed here

**Table 5** Temporal and directional variations in selenium concentrations (mg·kg$^{-1}$ d.w) in *Cedrus atlantica* wood tissues

| Age cluster | North | East | South | West | F-value | Mean |
|---|---|---|---|---|---|---|
| 2018–2022 | 77.13±1.64 eB | 33.33±0.64 efA | 33.40±1.17 aA | 34.66±1.42 cA | 872.6*** | 44.63±19.64 b |
| 2013–2017 | 77.40±1.90 eB | 28.09±0.93 bcA | 35.24±0.04 bA | 36.07±0.32 cA | 1408.3*** | 49.57±20.90 b |
| 2008–2012 | 41.03±0.40 dC | 32.28±0.17 aA | 35.56±0.34 bcB | 35.68±0.34 cB | 272.3*** | 35.09±4.83 a |
| 2003–2007 | 37.71±1.38 cC | 32.41±0.16 bcA | 35.92±0.47 bcdB | 34.96±0.34 cB | 27.1*** | 35.22±2.15 a |
| 1998–2002 | 37.36±0.93 cC | 32.07±0.18 bcdA | 35.88±0.66 bcdB | 35.70±0.86 cB | 25.2*** | 35.34±1.98 a |
| 1993–1997 | 37.11±0.75 bcC | 32.98±0.36 bA | 36.39±0.39 cdefBC | 35.53±0.60 cB | 54.2*** | 35.27±2.07 a |
| 1988–1992 | 36.29±0.69 abcC | 33.70±0.24 cdeA | 36.24±0.28 bcdeC | 34.84±0.93 cB | 18.7** | 35.09±1.51 a |
| 1983–1987 | 36.22±1.12 abcB | 33.08±0.22 efA | 36.91±0.56 defB | 35.65±0.36 cB | 13.0** | 35.62±1.37 a |
| 1978–1982 | 36.18±0.08 abcC | 33.51±0.30 deA | 37.00±0.19 efD | 35.27±0.20 cB | 260.8*** | 35.38±1.53 a |
| 1973–1977 | 35.04±0.97 aBC | 33.96±0.13 efB | 36.74±0.93 defC | 26.47±1.77 aA | 48.4*** | 32.94±4.19 a |
| 1968–1972 | 35.24±0.88 abB | 33.98±0.53 fB | 37.39±0.07 fC | 29.96±1.63 bA | 33.9*** | 34.14±2.94 a |
| 1963–1967 | 35.02±0.82 aB | 33.33±0.64 fB | 37.24±0.23 efC | 30.48±0.67 bA | 65.5*** | 34.18±2.60 a |
| F-value | 651.8*** | 45.7*** | 11.9*** | 31.6*** | | 3.7*** |

indicate significant historical Se input. From a mitigation perspective, the phytoremediation capacity of these species is significant. A mature tree containing wood with a Se concentration of ~70–90 mg·kg$^{-1}$ acts as a reservoir, allowing the long-term sequestration of grams of this pollutant and serving as a permanent sink. Therefore, although tree uptake does not directly reduce real-time air concentrations, strategically planting species with high Se accumulation capacity, such as *R. pseudoacacia* and *C. atlantica*, in highly polluted areas can make a significant contribution to nature-based mitigation strategies at the ecosystem level.

The study revealed that, in contrast to WD, Se levels in the OB were detectable across all examined species. This observation is predominantly attributable to the structural characteristics of the OB and its ability to accumulate particulate matter contaminated with heavy metals. Elevated Se concentrations in the OB indicate substantial Se pollution in the region under investigation (Cobanoglu et al. 2023; Kulac et al. 2025). Following contamination with heavy metals, airborne particulate matter roughens and cracks the OB surface, thereby facilitating particle adhesion.

In addition, Düzce province, where the study was conducted, is the 5th most polluted city in Europe (Koc et al. 2024). Studies conducted in the region have determined that the concentrations of heavy metals that can pose a threat to human health, such as Pb (Koç et al. 2025a), As (Yaşar İsmail et al. 2024), Sb (Canturk et al. 2024), Pd (Sevik et al. 2024), Bi (Isinkaralar et al. 2024), Cr (Pulatoglu et al. 2025), and Al (Koç et al. 2025b) are at very high levels. Moreover, it is stated that there is a robust and positive correlation between Se accumulated in wood and heavy metals such as Ag, Tl, Sb, As, Pb, and V, which induce adverse effects on human health even at low concentrations (Sevik et al. 2024). Thus, hazardous Se can be monitored using trees, a fact which is extremely important since their amounts can be evaluated retrospectively for decades, and long-term exposure can pose a threat to the environment and human health in the region (Şevik et al. 2024; Ulusoy and Mol 2022; Yabanli and Tay 2021).

The study findings generally indicate that the highest Se concentrations are observed in the northern direction. An explanation is that the samples from the north cardinal direction were collected near a major highway and an urban area in Türkiye. These findings suggest that Se pollution may be attributable to traffic or urban settlements (Şevik et al. 2024). Indeed, various studies have demonstrated that urban areas and vehicular traffic are among the primary sources of heavy metals. For example, in a survey conducted in Monte Carlo, it was determined that mixed metal smelting and transportation (30.72%) and coal combustion (25.21%) have more than 50% share in heavy metal pollution (Shi et al. 2024). In a study conducted in China, it was determined that the sources of heavy metals with the highest share were mixed (24.5%), industrial (24.8%), and building (24.7%) (Du et al. 2024). In Nanjing, it was determined that the primary sources of heavy metals/metaloids in particulate matter are traffic and industrial emissions, and these constitute 79.6% of the total variance (Ren et al. 2024). Based on our findings, the increased Se concentrations in the northern direction may be ascribed to traffic and urban influences.

Previous studies have demonstrated that the lowest concentrations of heavy metals are typically observed in WD compared with other organs, such as bark, leaves, and roots (Kuzmina et al. 2023; Akanbi et al. 2024). According to our study, the pattern of assimilation in urban parks may differ, as values were found in WD comparable to those in IB and OB. A relationship exists between WD location and heavy metal transfer. Wood is not connected to the external environment, but it absorbs chemical elements from the soil solution or transfers them between different tree organs through translocation (Pisarek et al. 2022). In industrial settings, less heavy metal accumulation occurs in WD sections than in bark or leaves, which are directly exposed to contamination. This is because metal transfer is time-dependent, and environmental factors can influence metal absorption (Dinh et al. 2019). The transport of elements in the WD is primarily mediated by the sapwood cell structure, particularly the cell wall (apoplastic pathway). The apoplastic membrane barrier is a flexible structure that detects and transmits signals in response to metal and metalloid stress (Chao and Chao 2025). Ion exchange capacity determines the number of metal ions that can be adsorbed onto biomaterials, which is strongly dependent on the valence of the metal species. (Pulatoglu et al. 2025). The potential of each tree to accumulate different heavy metals in its organs is different (Nechita et al. 2025c; Yiğit 2024).

Our study found that *R. pseudoacacia* WD showed consistent Se accumulation across directions (66.40–91.92 mg·kg$^{-1}$), suggesting either regulated physiological uptake mechanisms or uniform atmospheric deposition. Similar to *R. pseudoacacia*, the *C. atlantica* assimilated high amounts of Se in WD. Wood samples reached approximately 91.9 mg·kg$^{-1}$ in *R. pseudoacacia* and 77.4 mg·kg$^{-1}$ in *C. atlantica*, with northern exposures accumulating higher Se than eastern direction, suggesting either enhanced deposition or species-specific physiological uptake mechanisms. The pronounced directional variation in Se accumulation, particularly in *C. atlantica* (north > south = west = east), may also reflect wind-driven deposition patterns. Considering Düzce's dominant northeast-southwest winds and its bowl-shaped topography, it is probable that airborne Se-contaminated particulates tend to accumulate preferentially on windward-facing surfaces. The significantly higher Se concentrations in northern exposures (77.40 mg·kg$^{-1}$) vs. east

(28.09 mg·kg$^{-1}$) suggest that pollutants are transported and deposited by northeasterly winds, which dominate during high-pollution periods (late autumn/winter). These findings align with studies indicating that wind direction and speed significantly affect the deposition of particulate-bound metals on tree surfaces, especially where bark textures are rougher (e.g., *C. atlantica*), trapping more particulates (Liu et al. 2022; Cobanoglu et al. 2023; Pulatoglu et al. 2025). Conversely, the lower Se levels observed in eastern and western exposures may indicate leeward sheltering or the resuspension of finer particles under weaker winds. These dynamics highlight that local microclimatic conditions—rather than emission sources alone—determine the spatial variability in tree-based Se accumulation.

High Se concentrations in *R. pseudoacacia* and *C. atlantica* woods contrast with values reported for other tree species, as they slightly exceed 4.7 mg·kg$^{-1}$ in *Pinus nigra* WD (Sevik et al. 2025) and are around 3.7 mg·kg$^{-1}$ in *Pinus brutia* roots (Cebi Kilicoglu 2024). According to these results, *R. pseudoacacia* and *C. atlantica* are suitable species for reducing Se pollution, as they assimilate the highest Se concentrations. Moreover, they exhibit the lowest variability in metal deposition directionality, indicating that metals can be deposited relatively homogeneously within the wooden tree structure. Wood is the largest organ of trees and can absorb and accumulate heavy metals for decades or throughout a tree's entire lifespan, thereby substantially mitigating heavy metal pollution. Research has shown that heavy metals trapped in wood remain until the wood decays (Şevik et al. 2024).

Through our investigation, it was determined that Se concentrations in woods generally remained below detectable limits, as in *T. tomentosa*, *P. menziesii*, and *F. excelsior*, or varied within a narrow range. In contrast, Se concentrations between neighboring age clusters in *R. pseudoacacia*, which accumulate the highest Se levels in its WD, did not differ significantly, indicating high bioavailability, transfer, and translocation. This result suggests that Se can be relocated in WD from soil and air via root and foliar systems and bark deposition.

Although Se is not an essential element for plants, it is a semi-metallic element that can have beneficial effects on growth, antioxidant defense, and stress tolerance at low concentrations, but may become toxic at high levels. Se exists in inorganic and organic forms in nature. Inorganic forms include selenate ($SeO_2^{-4}$), selenite ($SeO_2^{-3}$), selenide ($Se_2^{-}$), and elemental Se. The major organic forms are SeCys and SeMet. Plant uptake of Se from soil depends largely on soil properties, the chemical form of Se, redox conditions, pH, and microbial activity in the rhizosphere. Plants primarily uptake Se from the soil through their roots, and the solubility and anionic form of Se play a decisive role in this process. While selenite taken up by the root is rapidly transported to the leaves via xylem flow, selenite is generally retained more in root tissues, and its transport to the xylem is more limited (Li et al. 2008; Hawrylak-Nowak 2009; Gupta and Gupta 2017; Schiavon and Pilon-Smits 2017; Hasanuzzaman et al. 2020). The transport of elements within the WD portion of plants is related mainly to the cell structure and, in particular, the cell wall (apoplastic pathway). The apoplast, located between the cell wall and the plasma membrane in plants, serves not only as an apoplastic membrane barrier but also as a flexible structure that senses and generates signals in response to metal/metalloid stress. The extent to which metal ions adsorbed to the sapwood remain available in these tissues likely depends on the ion exchange capacity of the xylem, and this capacity varies significantly by tree species (Pulatoglu et al. 2025).

Furthermore, it is challenging to observe high variability in tree-ring sections from the IB to the pith. A translocation jump between sapwood and hardwood is not evident for *R. pseudoacacia*, but can be discussed in the case of *C. atlantica* and *T. tomentosa*. Both *R. pseudoacacia* and *C. atlantica* are suitable for biomonitoring because they are sensitive to changes in atmospheric heavy metal pollution, accumulate metals in their tissues, and persist despite exposure to contaminants (Cobanoglu et al. 2023; Koc et al. 2024).

Our results indicate a significant difference in Se concentrations between neighboring cell groups in *C. atlantica*. *C. atlantica*, even if it absorbs lower amounts of metal in WD sections than *R. pseudoacacia*, can be considered the best species for biomonitoring changes in Se concentration resulting from the air deposition. Therefore, according to *C. atlantica* data, a sudden increase was observed in the west between 1978 and 1982 and again between 2013 and 2017, with this increase being much more pronounced in the north. Residential areas and highways are located in the north of the study area, while agricultural areas are located in the west. The migration and accumulation of Se in nature are complex processes that create a closed cycle among land, ocean, air, and organisms. Whether from human activities (e.g., coal combustion and mining) or from natural processes (e.g., volcanic eruptions and dust removal), Se is released into the atmosphere as selenium dioxide ($SeO_2$) and transported to other regions via precipitation and atmospheric deposition. Coal combustion is a primary source of Se. Other significant sources of Se include metal mining and smelting, coal, oil, and wood-burning, industrial activities, waste treatment, agricultural activities, car tires, engine wear, and incineration (Guo et al. 2024). This explains the sudden increase in Se concentration in the north after the 2013–2017 period, as observed in our study.

Because Düzce gained provincial status after the 1999 earthquake, and its population increased rapidly (Koç et al. 2025b). The increase to the west between 1978 and 1982 is attributed to agricultural activities. For *R. pseudoacacia*, micro-environmental conditions, such as wind-driven deposition, may predominate over tissue-specific uptake mechanisms; therefore, the accuracy of depicting Se metal retention in WD depends on the direction. *T. tomentosa*, *P. menziesii*, and *F. excelsior* have absorbed and retained low metal content in their tissues, making them unsuitable for phytoremediation.

## Conclusion and recommendations

This study provides critical insights into the use of urban trees for Se pollution management, demonstrating significant species-specific variation in accumulation capacity. *C. atlantica* is the only suitable biomonitor, showing distinct directional accumulation (45.39 mg·kg$^{-1}$ in northern exposures versus 32.52 mg·kg$^{-1}$ in eastern direction) and minimal inter-tissue translocation – essential traits for reliable pollution tracking. *R. pseudoacacia* proves most effective for phytoremediation with consistently high WD Se concentrations (66.40–91.92 mg·kg$^{-1}$) across all directions, while *C. atlantica* also shows promise (peak of 77.40 mg·kg$^{-1}$ in the north direction on age clusters). In north exposures, the OB of *T. tomentosa* (1.96 mg·kg$^{-1}$) and *F. excelsior* (2.20 mg·kg$^{-1}$) effectively indicate pollution levels, though their WD tissues accumulate minimally. Based on these findings, we recommend: (1) using *C. atlantica* exclusively for biomonitoring due to its directional sensitivity and stable sequestration, (2) planting *R. pseudoacacia* in high-pollution areas like highways for maximum Se uptake, (3) avoiding *P. menziesii* (OB: 0.52–1.04 mg·kg$^{-1}$) and *F. excelsior* for mitigation due to poor accumulation, and (4) investigating microclimatic factors behind the 2.7-fold north-east concentration difference in *C. atlantica* to optimize future urban planning strategies. These evidence-based recommendations leverage the quantified accumulation patterns to address monitoring and mitigation needs in polluted urban environments.

**Acknowledgements** We thank Kastamonu University Scientific Research Project Coordination for element analyses. C.N. extends gratitude for the support provided through Contract No. FORCLIMSOC 2023–2026, Projects PN 23090202 and 502 PN 23090302.

**Author contributions** Authors Contributions: İsmail Koç : design, raw material collection, data analysis, writing and reviewing. Hakan Sevik : design, data analysis, writing, and reviewing. Constantin Nechita : Writing, reviewing and editing. Ugur Canturk : Visualization, reviewing and editing. Andreea Maria Iordache : Reviewing and editing. J. Julio Camarero : Reviewing and editing and supervision. All authors read and approved the final manuscript.

**Funding** Open access funding provided by the Scientific and Technological Research Council of Türkiye (TÜBİTAK). Not applicable.

**Data availability** The data that support the findings of this study are available from the corresponding author upon reasonable request.

## Declarations

**Ethical approval** The author of this article has not conducted any studies involving human subjects or animals. The author has read, understood and complied with the "Ethical Responsibilities of Authors" statement in the Instructions for Authors.

**Consent to participate** Not applicable.

**Consent for publication** Not applicable.

**Clinical trial number** Not applicable.

**Competing interests** The authors declare no competing interests.



## References

Akanbi FS, Adamu UA, Olajide OS, Akun AS, Danyaya HA (2024) Comparative assessment of heavy metals loads in the shoot of selected tree plants and their accumulation potential in Kazaure, Jigawa Nigeria. Int J Latest Tech Eng Manage Appl Sci 13:102–110. https://doi.org/10.51583/IJLTEMAS.2024.130412

Ali MU, Liu G, Yousaf B, Ullah H, Abbas Q, Munir MAM (2019) A systematic review on global pollution status of particulate matter-associated potential toxic elements and health perspectives in urban environment. Environ Geochem Health 41:1131–1162. https://doi.org/10.1007/s10653-018-0203-z

Aricak B, Çetin M, Erdem R, Sevik H, Cometen H (2019) The change of some heavy metal concentrations in Scotch Pine (*Pinus sylvestris*) depending on traffic density, organelle and washing. Appl Ecol Environ Res 17. https://doi.org/10.15666/aeer/1703_67236734

Ayteğin A, Özcan M (2026) Assessment of heavy metal contamination in the Düzce watershed (Türkiye) and sustainable remedies through aquatic flora. BioResources 21(2):3021–3043. https://doi.org/10.15376/biores.21.2.3021-3043

Balraju W, Upadhyay KK, Dhyani R, Joshi R, Sharma A, Tripathi SK (2025) Dendrochemical analysis of heavy metals in Magnolia champaca tree rings in Mizoram, Northeast India. Environ Monit Assess 197:421. https://doi.org/10.1007/s10661-025-13903-z

Beloconi A, Vounatsou P (2023) Revised EU and WHO air quality thresholds: Where does Europe stand? Atmos Environ 314:120110. https://doi.org/10.1016/j.atmosenv.2023.120110

Canturk U, Koç İ, Ozel HB, Sevik H (2024) Identification of proper species that can be used to monitor and decrease airborne Sb pollution. Environ Sci Pollut Res 31:56056–56066. https://doi.org/10.1007/s11356-024-34939-7

Carvalho H (2021) New WHO global air quality guidelines: more pressure on nations to reduce air pollution levels. Lancet Planet Health 5:e760–e761. https://doi.org/10.1016/S2542-5196(21)00287-4

Cebi Kilicoglu M (2024) Metagenomic characterization of root fungal microbiota resistant to heavy metal stress in *Pinus brutia*. Water Air Soil Pollut 235:654. https://doi.org/10.1007/s11270-024-07468-9

Cesur A, Zeren Cetin I, Abo Aisha AES, Alrabiti OBM, Aljama AMO, Jawed AA et al (2021) The usability of *Cupressus arizonica* annual rings in monitoring the changes in heavy metal concentration in air. Environ Sci Pollut Res 28:35642–35648. https://doi.org/10.1007/s11356-021-13166-4

Çevre, Şehircilik ve İklim Değişikliği Bakanlığı (2023) Meteoroloji Genel Müdürlüğü. Türkiye Meteorolojik Afetler Değerlendirmesi (2010–2021) https://www.mgm.gov.tr/FILES/genel/raporlar/meteorolojikafetler2010-2021. pdf. 4

Chao Z-F, Chao D-Y (2025) Barriers and carriers for transition metal homeostasis in plants. Plant Commun 6(2):101235. https://doi.org/10.1016/j.xplc.2024.101235

Cobanoglu H, Sevik H, Koç İ (2023) Do annual rings really reveal Cd, Ni, and Zn pollution in the air related to traffic density? An example of the Cedar tree. Water Air Soil Pollut 234:65. https://doi.org/10.1007/s11270-023-06086-1

Dinh QT, Wang M, Tran TAT, Zhou F, Wang D, Zhai H et al (2019) Bioavailability of selenium in soil-plant system and a regulatory approach. Crit Rev Environ Sci Technol 49:443–517. https://doi.org/10.1080/10643389.2018.1550987

Du H, Lu X, Han X (2024) Spatial distribution characteristics and source apportionment of heavy metal(loid)s in park dust in the Mianyang urban area, China. Environ Geochem Health 46:104. https://doi.org/10.1007/s10653-024-01901-y

Erdem R, Aricak B, Cetin M, Sevik H (2023) Change in some heavy metal concentrations in forest trees by species, organ, and soil depth. Forestist 73(3):257–263. https://doi.org/10.5152/forestist.2023.22069

Erdem R, Koç İ, Çobanoglu H, Şevik H (2024) Variation of Magnesium, one of the macronutrients, in some trees based on organs and species. Forestist 74(1):84–93. https://doi.org/10.5152/forestist.2024.23025

Gan X, Huang J-C, Zhang M, Zhou C, He S, Zhou W (2021) Remediation of selenium-contaminated soil through combined use of earthworm *Eisenia fetida* and organic materials. J Hazard Mater 405:124212. https://doi.org/10.1016/j.jhazmat.2020.124212

Gogoi B, Acharjee SA, Bharali P, Sorhie V, Walling B (2024) A critical review on the ecotoxicity of heavy metal on multispecies in global context: A bibliometric analysis. Environ Res 248:118280. https://doi.org/10.1016/j.envres.2024.118280

Guney D, Koc I, Isinkaralar K, Erdem R (2023) Variation in Pb and Zn concentrations in different species of trees and shrubs and their organs depending on traffic density. Baltic For 29:id661. https://doi.org/10.46490/BF661

Guo K, Li, Wang J, Sui Z, Wang T, Pan WP (2024) A review on selenium in coal-fired power plants: Content and forms in coal, determination methods, migration, transformation, and control technologies. J Envir Chem Eng 12(5):113579. https://doi.org/10.1016/j.jece.2024.113579

Gupta M, Gupta S (2017) An overview of selenium uptake, metabolism, and toxicity in plants. Front Plant Sci 7:2074. https://doi.org/10.3389/fpls.2016.02074

Hadrup N, Ravn-Haren G (2020) Acute human toxicity and mortality after selenium ingestion: a review. J Trace Elem Med Biology 58:126435. https://doi.org/10.1016/j.jtemb.2019.126435

Hasanuzzaman M, Bhuyan MB, Raza A, Hawrylak-Nowak B, Matraszek-Gawron R, Al Mahmud J et al (2020) Selenium in plants: Boon or bane? Environ Exp Bot 178:104170. https://doi.org/10.1016/j.envexpbot.2020.104170

Hawrylak-Nowak B (2009) Beneficial effects of exogenous selenium in cucumber seedlings subjected to salt stress. Biol Trace Elem Res 132:259–269. https://doi.org/10.1007/s12011-009-8402-1

Haylock MR, Hofstra N, Klein Tank AMG, Klok EJ, Jones PD, New M (2008) A European daily high-resolution gridded data set of surface temperature and precipitation for 1950–2006. J Geophys Res-Atmos 113:D20. https://doi.org/10.1029/2008JD010201

He Y, Xiang Y, Zhou Y, Yang Y, Zhang J, Huang H et al (2018) Selenium contamination, consequences and remediation techniques in water and soils: A review. Environ Res 164:288–301. https://doi.org/10.1016/j.envres.2018.02.037

Huang Y, Song Y, Johnson D, Huang J, Dong R, Liu H (2019) Selenium enhanced phytoremediation of diesel contaminated soil by *Alternanthera philoxeroides*. Ecotoxicol Environ Saf 173:347–352. https://doi.org/10.1016/j.ecoenv.2019.02.040

Iordache AM, Nechita C, Voica C, Pluháček T, Schug KA (2022) Climate change extreme and seasonal toxic metal occurrence in Romanian freshwaters in the last two decades—case study and critical review. npj Clean Water 5:2. https://doi.org/10.1038/s41545-021-00147-w

IQAir (2024) World's most polluted cities. https://www.iqair.com/world-most-polluted-cities?cities=Evar8W6Rk9B2ycaMG. Accessed 10 Dec 2025

Irfeey AM, Chau H-W, Sumaiya MM, Wai CY, Muttil N, Jamei E (2023) Sustainable mitigation strategies for urban heat island effects in urban areas. Sustainability 15(14):10767. https://doi.org/10.3390/su151410767

Isinkaralar K, Isinkaralar O, Koç İ, Özel HB, Şevik H (2024) Assessing the possibility of airborne bismuth accumulation and spatial distribution in an urban area by tree bark: a case study in Düzce, Türkiye. Biomass Convers Bior 14:22561–22572. https://doi.org/10.1007/s13399-023-04399-z

Isinkaralar K, Isinkaralar O, Koç İ, Şevik H, Özel HB (2025a) Atmospheric trace metal exposure in a 60-year-old wood: A sustainable methodological approach to measurement of dry deposition. Int J Environ Re 19:112. https://doi.org/10.1007/s41742-025-00783-x

Isinkaralar O, Isinkaralar K, Sevik H (2025b) Health for the future: spatiotemporal CA-MC modeling and spatial pattern prediction via dendrochronological approach for nickel and lead deposition. Air Qual Atmos Health 18:1087–1099. https://doi.org/10.1007/s11869-025-01702-x

Jain H (2024) From pollution to progress: Groundbreaking advances in clean technology unveiled. Innov Green Dev 3:100143. https://doi.org/10.1016/j.igd.2024.100143

Key K, Kulaç Ş, Koç İ, Sevik H (2023) Proof of concept to characterize historical heavy-metal concentrations in atmosphere in North Turkey: determining the variations of Ni, Co, and Mn concentrations in 180-year-old *Corylus colurna* L. (Turkish hazelnut) annual rings. Acta Physiol Plant 45:120. https://doi.org/10.1007/s11738-023-03608-6

Koc I, Cobanoglu H, Canturk U, Key K, Kulac S, Sevik H (2024) Change of Cr concentration from past to present in areas with

elevated air pollution. Int J Environ Sci Tec 21:2059–2070. https://doi.org/10.1007/s13762-023-05239-3
Koç İ (2021) Changes that may occur in temperature, rain, and climate types due to global climate change: The example of Düzce. Turkish J Agric- Food Sc Tec 9:1545–1554. https://doi.org/10.24925/turjaf.v9i8.1545-1554.4467
Koç İ (2025) Chronological levels of As, Pd, V, and Sr in 356-year-old *Pinus nigra* annual rings in northern Türkiye. BioResources 20(1):2215–2233. https://doi.org/10.15376/biores.20.1.2215-2233
Koç İ, Cobanoglu H, Canturk U, Key K, Sevik H, Kulac S (2025a) Variation of 40-year Pb deposition in some conifers grown in the air-polluted-urban area of Düzce, Türkiye. Environ Earth Sci 84:186. https://doi.org/10.1007/s12665-025-12211-6
Koç İ, Canturk U, Cobanoglu H, Kulac S, Key K, Sevik H (2025b) Assessment of 40-year Al deposition in some exotic conifer species in the urban air of Düzce, Türkiye. Water Air Soil Pollut 236:76. https://doi.org/10.1007/s11270-024-07723-z
Kulac S, Pulatoglu AO, Koç İ, Sevik H, Ozel HB (2025) Assessing tree species for monitoring and mitigating strontium pollution in urban environments. Water Air Soil Pollut 236:605. https://doi.org/10.1007/s11270-025-08244-z
Kuzmina N, Menshchikov S, Mohnachev P, Zavyalov K, Petrova I, Ozel HB et al (2023) Change of aluminum concentrations in specific plants by species, organ, washing, and traffic density. BioResources 18(1):792–803. https://doi.org/10.15376/biores.18.1.792-803
Li H-F, McGrath SP, Zhao FJ (2008) Selenium uptake, translocation and speciation in wheat supplied with selenate or selenite. New Phytol 178:92–102. https://doi.org/10.1111/j.1469-8137.2007.02343.x
Liu G, Zhang Y, Qi C, Zheng L, Chen Y, Peng Z (2007) Comparative on causes and accumulation of selenium in the tree-rings ambient high-selenium coal combustion area from Yutangba, Hubei, China. Environ Monit Assess 133:99–103. https://doi.org/10.1007/s10661-006-9563-4
Liu H, Wang X, Zhang B, Han Z, Wang W, Chi Q et al (2021) Concentration and distribution of selenium in soils of mainland China, and implications for human health. J Geochem Expl 220:106654. https://doi.org/10.1016/j.gexplo.2020.106654
Liu Y, Zhao X, Liu R, Zhou J, Jiang Z (2022) Biomonitoring and phytoremediation potential of the leaves, bark, and branch bark of street trees for heavy metal pollution in urban areas. Environ Monit Assess 194:344. https://doi.org/10.1007/s10661-022-10004-z
Liu Y, Xu F, Liu W, Liu X, Wang D (2025) Characteristics, sources, exposure, and health effects of heavy metals in atmospheric particulate matter. Curr Pollut Rep 11:16. https://doi.org/10.1007/s40726-025-00344-y
Matei E, Râpă M, Mateș IM, Popescu AF, Bădiceanu A, Balint AI, Covaliu-Mierlă CI (2025) Heavy metals in particulate matter—Trends and impacts on environment. Molecules 30(7):1455. https://doi.org/10.3390/molecules30071455
Mutlu E, Tokatlı C, Islam ARMT, Islam MS, Muhammad S (2024) Water quality assessment of Şehriban stream (Kastamonu, Türkiye) from a multi-statistical perspective. Int J Environ Anal Chem 104:8229–8245. https://doi.org/10.1080/03067319.2023.2197114
Nechita C, Iordache AM, Lemr K, Levanič T, Pluhacek T (2021) Evidence of declining trees resilience under long term heavy metal stress combined with climate change heating. J Clean Prod 317:128428. https://doi.org/10.1016/j.jclepro.2021.128428
Nechita C, Iordache AM, Pluhacek T, Gregar F, Camarero JJ (2025a) Hazardous metals coupled with increasing summer diurnal temperature range contributed to growth decline of two oak species in a heavily industrialized area. J Hazard Mat 496:139519. https://doi.org/10.1016/j.jhazmat.2025.139519
Nechita C, Iordache AM, Roba C, Sandru C, Zgavarogea R, Camarero JJ (2025b) Non-linear relationships between climate and toxic metals in stressed polluted areas. Environ Res 287:123124. https://doi.org/10.1016/j.envres.2025.123124
Nechita C, Iordache AM, Roba C, Sandru C, Zgavarogea R, Camarero JJ (2025c) Heavy metal health risk assessment in *Picea abies* L. forests along an altitudinal gradient in Southern Romania. Plants 14(6):968. https://doi.org/10.3390/plants14060968
Pisarek P, Bueno M, Thiry Y, Legout A, Gallard H, Le Hécho I (2022) Influence of tree species on selenium and iodine partitioning in an experimental forest ecosystem. Sci Total Environ 809:151174. https://doi.org/10.1016/j.scitotenv.2021.151174
Pulatoglu AO, Koç İ, Özel HB, Şevik H, Yıldız Y (2025) Using trees to monitor airborne Cr pollution: Effects of compass direction and woody species on Cr uptake during phytoremediation. BioResources 20:121. https://doi.org/10.15376/biores.20.1.121-139
Ren Y, Hu Y, Cheng H (2024) Sources, bioaccessibility and health risk of heavy metal(loid)s in the particulate matter of urban areas. Sci Total Environ 947:174303. https://doi.org/10.1016/j.scitotenv.2024.174303
Saxena V (2025) Water quality, air pollution, and climate change: Investigating the environmental impacts of industrialization and urbanization. Water Air Soil Pollut 236:73. https://doi.org/10.1007/s11270-024-07702-4
Schiavon M, Pilon-Smits EAH (2017) The fascinating facets of plant selenium accumulation – biochemistry, physiology, evolution and ecology. New Phytol 213:1582–1596. https://doi.org/10.1111/nph.14378
Sevik H, Cetin M, Ozel HB, Akarsu H, Zeren Cetin I (2019a) Analyzing of usability of tree-rings as biomonitors for monitoring heavy metal accumulation in the atmosphere in urban area: a case study of cedar tree (*Cedrus* sp). Environ Monit Assess 192:23. https://doi.org/10.1007/s10661-019-8010-2
Sevik H, Ozel HB, Cetin M, Özel HU, Erdem T (2019b) Determination of changes in heavy metal accumulation depending on plant species, plant organism, and traffic density in some landscape plants. Air Qual Atmos Health 12:189–195. https://doi.org/10.1007/s11869-018-0641-x
Sevik H, Koç İ, Cobanoglu H (2024) Determination of some exotic landscape species as biomonitors that can be used for monitoring and reducing pd pollution in the air. Water Air Soil Poll 235:615. https://doi.org/10.1007/s11270-024-07429-2
Sevik H, Koç İ, Cregg B, Nzokou P (2025) Tissue-specific barium accumulation in five conifer species: a 40-year dendrochemical assessment from a polluted urban environment. Environ Geochem Health 47:356. https://doi.org/10.1007/s10653-025-02679-3
Şevik H, Yildiz Y, Özel HB (2024) Phytoremediation and long-term metal uptake monitoring of silver, selenium, antimony, and thallium by Black pine (Pinus nigra Arnold). BioResources 19(3):4824–4837. https://doi.org/10.15376/biores.19.3.4824-4837
Shi J, Yang Y, Shen Z, Lin Y, Mei N, Luo C et al (2024) Identifying heavy metal sources and health risks in soil-vegetable systems of fragmented vegetable fields based on machine learning, positive matrix factorization model and Monte Carlo simulation. J Hazard Ma 478:135481. https://doi.org/10.1016/j.jhazmat.2024.135481
Şimşek A, Mutlu E (2023) Assessment of the water quality of Bartın Kışla (Kozcağız) Dam by using geographical information system (GIS) and water quality indices (WQI). Environ Sci Pollut Res 30:58796–58812. https://doi.org/10.1007/s11356-023-26568-3
Swain CK (2024) Environmental pollution indices: a review on concentration of heavy metals in air, water, and soil near industrialization and urbanisation. Discov Environ 2:5. https://doi.org/10.1007/s44274-024-00030-8

Ullah H, Lun L, Rashid A, Zada N, Chen B, Shahab A et al (2023) A critical analysis of sources, pollution, and remediation of selenium, an emerging contaminant. Environ Geochem Health 45:1359–1389. https://doi.org/10.1007/s10653-022-01354-1

Ulusoy Ş, Mol S (2022) Trace elements in seabass, farmed by Turkey, and health risks to the main consumers: Turkish and Dutch populations. Environ Monit Assess 194:224. https://doi.org/10.1007/s10661-022-09806-y

Uncumusaoğlu AA, Mutlu E (2021) Water quality assessment in Karaboğaz Stream Basin (Turkey) from a multi-statistical perspective. Pol J Environ Stud 30(5):4747–4759. https://doi.org/10.15244/pjoes/132909

Vasconcellos TJd S, dos RSd MJ, Tomazello-Filho M, Callado CH (2025) Recording chemical changes in an urban environment: A dendrochemical study of Ceiba speciosa (A. St.-Hil.) Ravenna (Malvaceae) in the Atlantic Forest. Dendrochronologia 89:126286. https://doi.org/10.1016/j.dendro.2024.126286

Winkel LHE, Vriens B, Jones GD, Schneider LS, Pilon-Smits E, Bañuelos GS (2015) Selenium Cycling Across Soil-Plant-Atmosphere Interfaces: A Critical Review. Nutrients 7(6):4199–4239. https://doi.org/10.3390/nu7064199

Yabanli M, Tay S (2021) Selenium and mercury balance in sea bream obtained from different living environments in Turkey: a risk assessment for the consumer health. Environ Sci Pollut Res 28:36069–36075. https://doi.org/10.1007/s11356-021-13366-y

Yang J, Ma J, Sun Q, Han C, Guo Y, Li M (2022) Health benefits by attaining the new WHO air quality guideline targets in China: A nationwide analysis. Environ Pollut 308:119694. https://doi.org/10.1016/j.envpol.2022.119694

Yaşar İsmail TS, İsmail MD, Çobanoğlu H, Koç İ, Sevik H (2024) Monitoring arsenic concentrations in airborne particulates of selected landscape plants and their potential for pollution mitigation. Forestists 75:1–6. https://doi.org/10.5152/forestist.2024.24071

Yiğit N (2024) Determination of sixteen woody species' ability to sequester Sr, Mo, and Sn pollutants. BioResources 19(4):784. https://doi.org/10.15376/biores.19.4.7842-7855

Yuan Z, Cai S, Yan C, Rao S, Cheng S, Xu F et al (2024) Research Progress on the Physiological Mechanism by Which Selenium Alleviates Heavy Metal Stress in Plants: A Review. Agronomy 14(8):1787. https://doi.org/10.3390/agronomy14081787

Zeren Çetin İ (2024) Used in urban area for landscape planning and design spatial and temporal variations in chromium (Cr) concentrations in *Picea orientalis* L. Turkish J Agric- Food Sci Tec 12:1730–1738. https://doi.org/10.24925/turjaf.v12i10.1730-1738.7093

Ziaeemehr B, Jandaghian Z, Ge H, Lacasse M, Moore T (2023) Increasing solar reflectivity of building envelope materials to mitigate urban heat islands: State-of-the-Art Review. Buildings 13(11):2868. https://doi.org/10.3390/buildings13112868

Zou S, Mauter MS (2021) Direct electrochemical pathways for selenium reduction in aqueous solutions. ACS Sustain Chem Eng 9(5):2027–2036. https://doi.org/10.1021/acssuschemeng.0c06585